CHAPTER 16

Resonances of Coastal Waters Between Perth and Geraldton (Western Australia)

H. ALLISON, Ph.D. M.Sc., MIE Aust., M.R. Soc (Vic. & W.A.), Senior Research Scientist, CSIRO, Div. of Land Resources Management, Wembley, 6014.
A. GRASSIA, Dr. Math. & Phys., B.A. Principal Research Scientist, CSIRO, Div. of Mathematics and Statistics, Wembley, 6014.
R. LITCHFIELD, CSIRO, Div. of Mathematics and Statistics, Wembley, 6014.

SUMMARY Sea-level oscillations along the Western Australian coast, with periods in the range of 20-40 mins, have considerably greater amplitudes between Perth and Geraldton than at other locations along the coastline. It is shown that amplification of these oscillations is due to resonance in the near shore basin formed by the shore and a submerged reef-chain parallel to and 5 km from the shore.

The rigorous analytical solution for the resonance frequencies is obtained for the two-dimensional hydrodynamic model. Comparison with results from spectral analysis of recorded oscillations indicates a satisfactorily agreement with the theory. Statistical estimation of damping of the observed oscillations indicates that the predominant resonance in the first mode is sharp, having the quality factor Q=10.

1 Introduction

Nearshore sea-level oscillations, apart from tides, are observed at many locations. The oscillations have periods ranging from several minutes (surf beat, nearshore edge waves, harbour seiches) through several hours (continental shelf waves) to hundreds of days (planetary waves) (Le Blond and Mysak, 1978). Research on continental shelf waves in Western Australia (Hamon, 1966) initiated world-wide theoretical and experimental study of the subject. Later studies by Hamon (1976) indicated that the shelf waves in Australia were generated by wind, supporting the point of view of Gill and Schumann (1974). Recently sea-level oscillations along the Western Australian coastline, with periods in the range 20-40 min, were reported by Allison and Grassia (1979) to be attributed to the presence of a reef-chain parallel and 5 km from the Western Australian shore (Fig. 1).

The new results are reported below, including the spectral analysis of sea-level oscillations, theoretical solutions for the two-dimensional hydrodynamic model, which in particular indicates the presence of oscillating currents near the coastline.

2 Long-term statistics

Western Australian tidal records for the last 15 years were analysed. On many of them, short period (relative to tidal period) oscillations

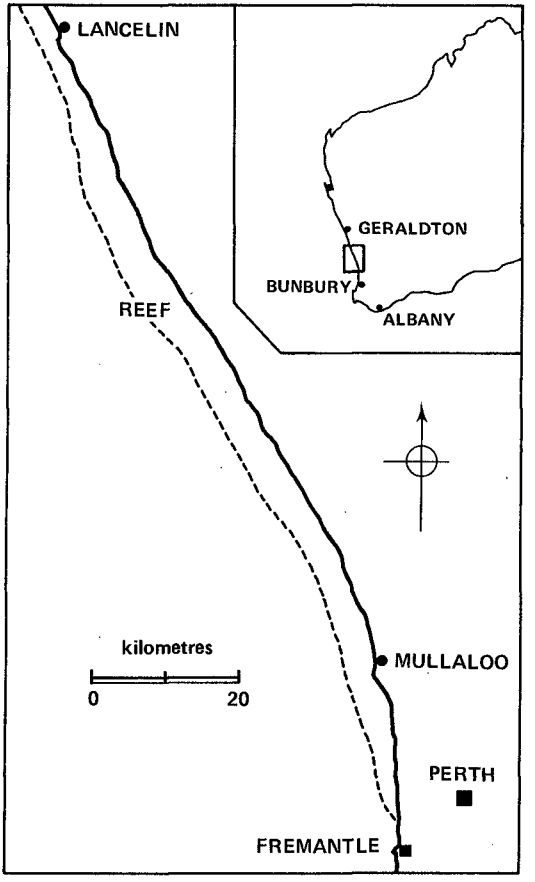

Figure 1. Submerged Reef Chain Off Western Australian Coast

were present. These oscillations usually were of small amplitudes, of the order of several centimetres. However, occasionally large amplitude oscillations occurred and lasted several hours, sometimes persisting for one or two days (with corresponding smaller amplitudes). A typical such sporadic oscillation is presented in Figure 2.

In the following any sea-level oscillation, having its amplitude $\geq$ 10cm is called an event. In total, 219 such events were observed between 1963 and 1978.

To characterise the intensity of the event we have used its energy E, which was calculated on the basis of the following formula:

$$E = \frac{\rho g A^2 \tau}{4T} \tag{1}$$

which follows from the familiar expression of a maximum energy of a standing wave per unit surface and per one cycle of oscillations of the period T:

$$E_T = \frac{1}{4} \rho g A^2 \tag{2}$$

Here ρ is the mass density of water, g is a gravity acceleration, A was taken as a maximum amplitude during the sea-level oscillation event, and τ is a duration of the oscillation event, which was taken as a length of time during which amplitudes of oscillations exceeded the threshold value of 10cm.

Estimate of energy obtained by (1) is, of course, exaggerated, because the formula is valid, strictly speaking, only for waves, sinusoidal in time, while the recorded oscillations decay with time (Fig. 2). A justification of its use is however simple: we are interested only in relative variation of the energy of the events in the long term, rather than in the absolute value of the energy.

To characterise the probability of occurrence of large sea-level oscillation events we used their frequency of appearance, meaning number of events occurring during a certain selected interval, such as a month or a year. (Notice that on the following pages we shall also use the word 'frequency' in the physical sense, such as 'resonance frequency', not to be confused with the statistical frequency of occurrence).

The results of calculations of seasonal and yearly variations of event frequencies and energies are shown in Fig. 3 and 4. (In Fig. 4 the yearly averages of Zürich sunspot numbers are shown for comparison).

The monthly averages (Fig. 3) indicate that more events and events with larger energy occur in the Southern Hemisphere winter. This may indicate that observed events are possibly caused by long waves, generated by winter storms in the Indian Ocean, but we do not possess any independent proof of this.

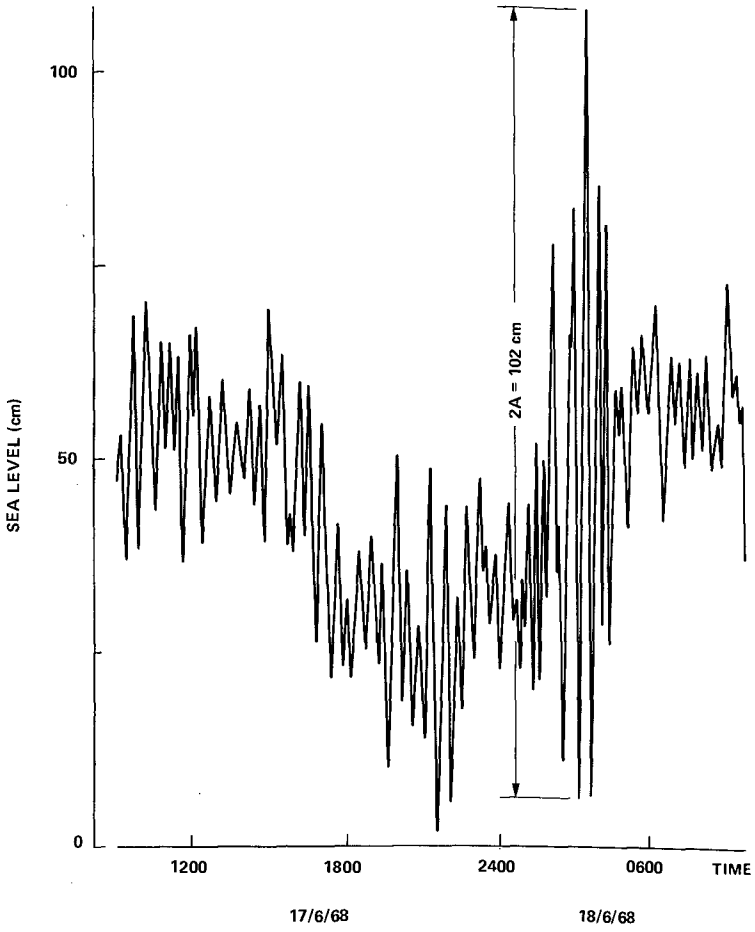

Figure 2. Tidal Record Geraldton, W.A.

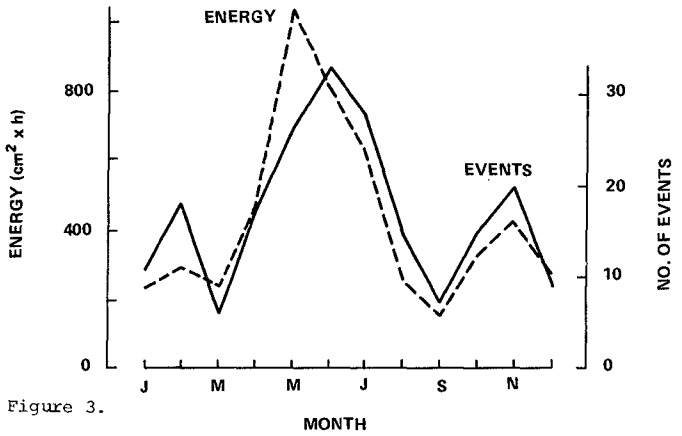

Figure 3.

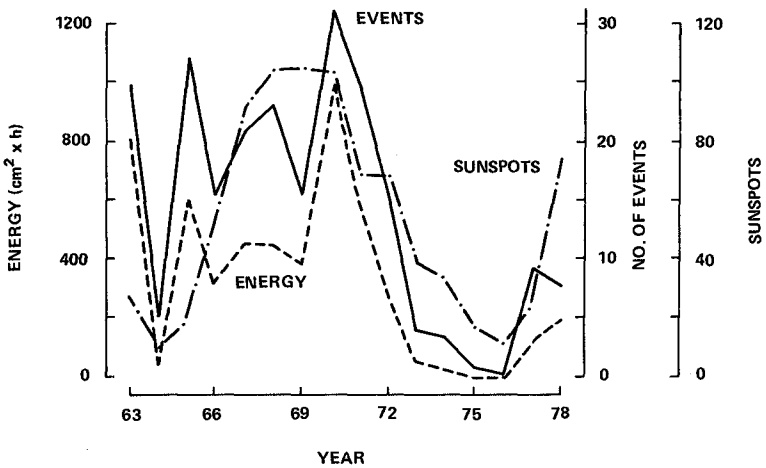

Figure 4. Monthly and Yearly Frequencies of Events

The yearly averages demonstrate a remarkable resemblance to the solar activity pattern (in fact, our calculations had shown a statistically significant correlation of the energies and frequencies of occurrence of events to solar activity). However, in spite of some recent claims about solar-terrestial relationship (see, for example, Currie, 1976) we are reluctant to speculate here on the subject, leaving room for further study, which might, possibly, indicate the correlation between storms in the Indian Ocean and solar activity.

3 Short-term statistics - spectral analysis

The large sea-level oscillation event, described above, usually occur on the background of small amplitude oscillations. These small oscillations, (with the amplitudes below threshold of 10cm) are persistent practically always, and generate permanently present oscillating currents in the nearshore zone of Western Australia.

An example of such small amplitude oscillations is shown in Fig. 5.

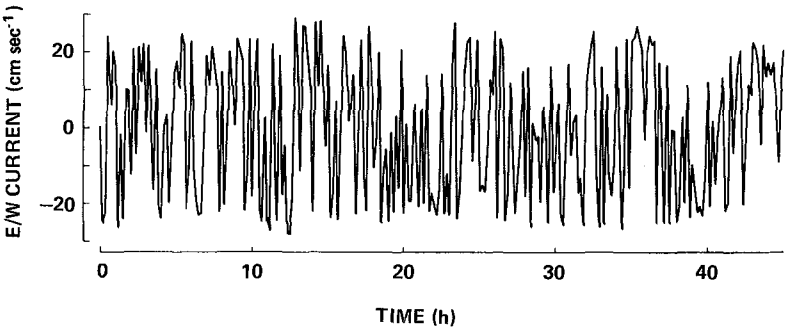

Figure 5 Small Oscillations of East-West Current, Mullaloo, W.A.

While it has been proved (Allison and Grassia, 1979) that large sea-level oscillations events are associated with the standing waves between the shore and the reef-chain, no such proof has been made for small amplitude background oscillations. We present here some evidence in support of the point of view, that these always persistent small amplitude oscillations originate in the same way as the large ones. To this point, let us consider the results of spectral analysis of both large sea-level oscillations and small-amplitude background. These results are presented correspondingly on Fig. 6a,b.

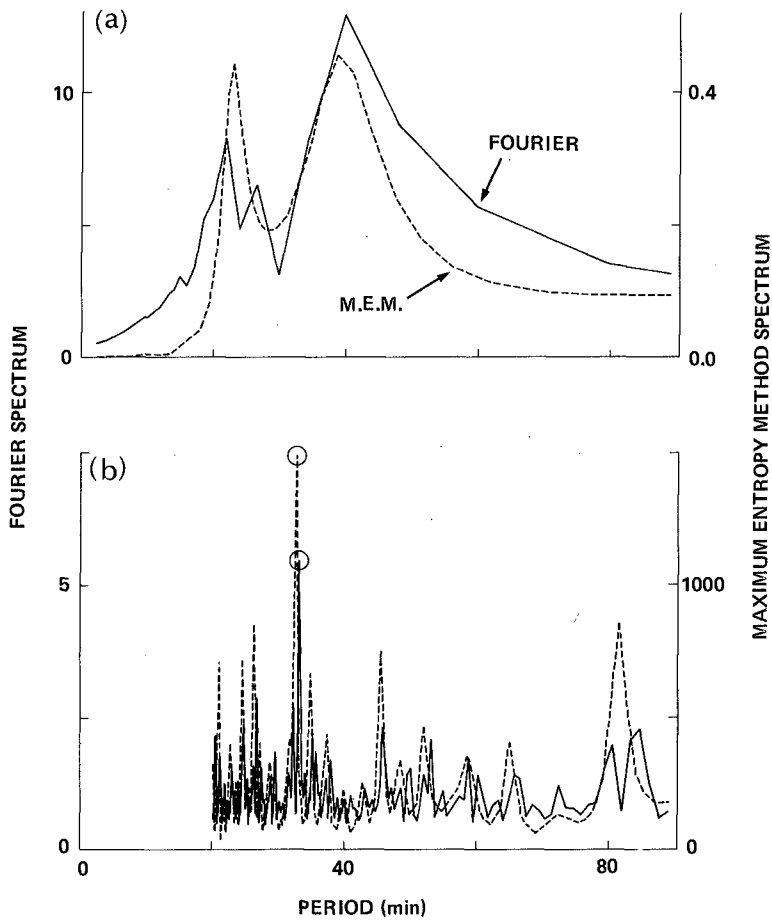

Figure 6. Period Spectrum of:
(a) Large Oscillations (b) Small Oscillations

The solid lines on both parts (a) and (b) of Fig. 6 correspond to the modulus of the Fourier Spectrum of the oscillations, the dashed lines show the Maximum Entropy Method spectra. It is seen, first of all, that the Maximum Entropy Method gives results, closely corresponding to the ordinary Fourier Analysis, although some spurious peaks, given by Fourier Analysis are effectively suppressed by the Maximum Entropy Method. Most important, however, is the presence of considerably sharp resonance peaks on both spectra.

The comparison of computed resonance periods for large sea-level oscillation events and small-amplitude background is given in Table 1.

Table 1

	Distance from reef to shore	Dominant Period	Non-dimensional Frequency
	ℓ (km)	T (mins)	$R = \frac{2\pi \ \ell}{T \sqrt{gh}}$ ... (18)
Large oscillations Geraldton, W.A.	5	40	1.32
Small oscillations Mullaloo, W.A.	4.5	33	1.44

As seen from Table 1, the non-dimensional frequencies of large and small oscillations are in reasonable agreement, thus substantiating the point of view, that both types of oscillations are, in essence, resonances in a hydrodynamic system, namely, the basin formed by the shore and nearshore reef chain. We consider now the analytical treatment of the resonances.

4 Analytical Development

The bottom topography of the nearshore basin is represented by the dashed area in Fig. 7. We approximate this profile by the parabolic expression

$$h(x) = h_o \left[1-\left(\frac{x}{\ell}\right)^2 (1-\alpha)\right] \qquad (3)$$

where h_o refers to the depth at $x=0$, ℓ being the length of the basin (in our case the width of the channel) and α is a non-dimensional parameter, describing the fact that the reef-chain is submerged. For the values h_o = 10m; α = 0.3 the graph of expression (3), shown by a solid line in Fig. 7, provides an idealised smooth representation of the bottom profile. The chief advantage of using (3) is that it allows us to obtain a rigorous analytical solution of the equation of water motion in the basin partly open to the ocean. One may notice that variation in the parameter α permits also consideration of various cases of submergency of the reef.

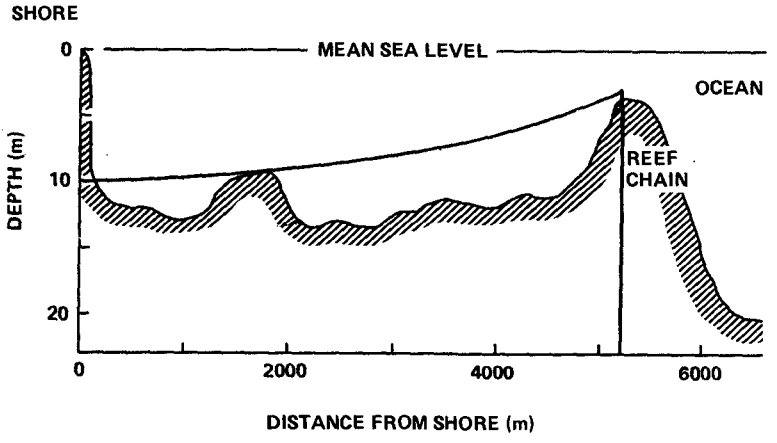

Figure 7 Typical Bottom Topography in W.A. (normal to shore)

When $\alpha = 1$ the basin has a uniform depth with one end (x=0) closed and the other end (x=ℓ) opened into the deep ocean, being the classical problem, for which the exact solutions are known (Lamb, 1932). When $\alpha = 0$, we have the closed basin with a parabolic bottom profile, being the other classical case (Chrystal, 1904).

We give below the rigorous solution for the intermediate case of a partly open basin with the parabolic bottom for $0 \leq \alpha \leq 1$: the classical problems, considered by Chrystal and Lamb emerging as the limiting cases of the solution that follows. As the depth is in the order of 10m, while length of the basin (width of the channel) is in the range 4-6 km, we accept as a starting point the familiar shallow water equation:

$$g \frac{\partial}{\partial x} [h(x) \frac{\partial \eta}{\partial x}] = \frac{\partial^2 \eta}{\partial t^2} \tag{4}$$

where g is a gravity acceleration and η (x,t) represents the elevation of the free surface of water above its undisturbed surface level.

Considering free oscillations with frequency ω, we, as usual, represent η (x,t) as a product of two functions, one describing the shape of water motion $\xi(x)$ and the other being a time-dependent term $e^{-i\omega t}$.

$$\eta(x,t) = \xi(x) e^{-i\omega t} \tag{5a}$$

The second time derivative becomes:

$$\frac{\partial^2}{\partial t^2}\,\eta(x,t) = -\,\xi(x)\; e^{-i\omega t}\;\omega^2. \tag{5b}$$

After the separation of variables, and substitution of h(x) as in (3), eq. (4) takes the form:

$$\frac{d^2\xi}{dx^2}\,[1-(\frac{x}{\ell})^2(1-\alpha)] - \frac{d\xi}{dx}\,[\frac{2x}{\ell^2}\,(1-\alpha)] + \frac{\omega^2}{gh_o} = 0. \tag{6}$$

Introducing the new variable

$$z^2 = (\frac{x}{\ell})^2\,(1-\alpha) \tag{7}$$

we obtain the following sequence of simple formulae:

$$z = (\frac{x}{\ell})\;(1-\alpha)^{1/2}\quad;\quad \frac{dx}{dz} = \ell\;(1-\alpha)^{-1/2}\qquad\} \tag{8a}$$

$$x = z\ell\;(1-\alpha)^{-1/2}\quad;\quad \frac{d^2x}{dz^2} = 0\qquad\}$$

$$\frac{d\xi}{dx} = (\frac{dx}{dz})^{-1}\,\frac{d\xi}{dz} = (1-\alpha)^{1/2}\ell^{-1}\,\frac{d\xi}{dz}\qquad\} \tag{8b}$$

$$\frac{d^2\xi}{dx^2} = (\frac{dx}{dz})^{-2}\,\frac{d^2\xi}{dz^2} - (\frac{d^2x}{dz^2})\;(\frac{dx}{dz})^{-3}\,\frac{d\xi}{dz} = (1-\alpha)\ell^{-2}\,\frac{d^2\xi}{dz^2}\;\}$$

Substitution of (8a), (8b) and (7) in (6) leads to the following equation:

$$(1-z^2)\,\frac{d^2\xi}{dz^2} - 2z\,\frac{d\xi}{dz} + \frac{\omega^2\ell^2}{gh_o\,(1-\alpha)}\,\xi = 0 \tag{9}$$

which has the familiar form of a Legendre equation, if we put

$$\frac{\omega^2\ell^2}{gh_o\,(1-\alpha)} = n\,(n+1) \tag{10}$$

where the integer n, being a mode number, takes the values 1,2,3...

The general solution of (9) with the notation (10) has a form:

$$\xi(z) = AP_n(z) + BQ_n(z) \tag{11}$$

where A and B are arbitrary constants and $P_n(z)$ and $Q_n(z)$ are the Legendre functions, of which $P_n(z)$ is always a polynomial, but $Q_n(z)$ is not. Let us consider initially the boundary condition at the shore side of the basin, where no current is possible. This can be written as a condition on the first derivative of the vertical displacement ξ, at the point $x = z = 0$:

$$\frac{d\xi}{dz}\Big|_{z=0} = 0 \tag{12}$$

which, after substitution of (11) into (12) becomes:

$$\frac{d\xi}{dz}\Big|_{z=0} = AP_n'(0) + BQ_n'(0) = 0 \tag{13}$$

We can utilize now the useful properties of the Legendre functions, given in the Table 2.

Table 2

For even n	For odd n
$P_n'(0) = Q_n(0) = 0$	$P_n(0) = Q_n'(0) = 0$
$P_n(0) \neq 0$; $Q_n'(0) \neq 0$	$P_n'(0) \neq 0$; $Q_n(0) \neq 0$

Substituting the values from Table 2 into eq. (11) we obtain that the solutions, satisfying the boundary condition (12) are:

$$\xi = AP_n(z) \qquad \text{(n even)} \tag{14a}$$

$$\xi = BQ_n(z) \qquad \text{(n odd)} \tag{14b}$$

Explicit expressions for the first six solutions are given below:

$$P_o(z) = 1$$

$$Q_1(z) = \frac{z}{2} \ln \frac{1+z}{1-z} - 1 \tag{15}$$

$$P_2(z) = \frac{1}{2}(2z^2-1) \qquad \text{(15 cont.)}$$

$$Q_3(z) = \left(\frac{5z^3}{4} - \frac{3z}{4}\right) \ln\frac{1+z}{1-z} - \frac{5}{2}z^2 + \frac{2}{3}$$

$$P_4(z) = \frac{1}{8}(35z^4 - 30z^2 + 3)$$

$$Q_5(z) = \left(\frac{63}{16}z^5 - \frac{70}{16}z^3 + \frac{15}{16}z\right) \ln\frac{1+z}{1-z} - \frac{63}{8}z^4 + \frac{49}{8}z^2 - \frac{8}{15}$$

$$P_6(z) = \frac{1}{16}(231z^6 - 315z^4 + 105z^2 - 5)$$

These solutions and also the solutions of any desirable higher orders can be obtained by use of the recurrence relations (Abramowitz and Stegun, 1975).

$$(n+1)P_{n+1}(z) = (2n+1)zP_n(z) - nP_{n-1}(z) \qquad (16a)$$

$$(n+1)Q_{n+1}(z) = (2n+1)zQ_n(z) - nQ_{n-1}(z) \qquad (16b)$$

by starting from $P_o(z)$, $Q_1(z)$ as in (13) and using:

$$P_1(z) = z; \quad Q_o(z) = \frac{1}{2}\ln\frac{1+z}{1-z} \qquad (17)$$

The domain of definition of the functions (15) in our problem is within $0 \leq z \leq (1-\alpha)^{1/2}$, as it follows from eq. (8). The solutions (15) within the mentioned domain of definition give for any selected n the shape of possible modes of oscillations of water in the basin, the corresponding angular frequencies being determined from (10) depending once again on the integer n.

It is convenient to introduce the non-dimensional frequency parameter R, which, as follows from (10), is equal:

$$R = \frac{\omega\ell}{(gh_o)^{1/2}} = [(1-\alpha)n(n+1)]^{1/2} \qquad (18)$$

If the basin would be of constant depth h_o, the parameter R will take the following values:

$$R_o = \{\ \pi/2;\ 3\pi/2;\ 5\pi/2 \ \ldots\ (2k-1)\ \pi/2\ \} \qquad (19a)$$

$$R_c = \{\ \pi;\ 2\pi;\ 4\pi;\ \ldots\ 2k\pi\ \} \qquad (19b)$$

Here R_o refers to the basin open to the ocean ($\alpha = 1$); R_c refers to the closed basin ($\alpha = 0$).

In our case of a parabolic bottom the parameter R can be calculated by the use of (18). The results, giving R as a function of α and various values of n, are plotted in Fig. 8, where the values of R, as in (19), for constant water depth are shown by horizontal dashed lines. Open dots on the graphs $R_n(\alpha)$ indicate the positions of the first and second zeroes of the Legendre P_{2j}, Q_{2j-1} (j=1,2,3) functions, the solid lines marked Z_1 and Z_2, joining the zeroes, show the tendency of the zeroes to approach the limiting values of $R = \pi/2;\ 3\pi/2$ for $\alpha \to 1$, as from (19a), for $n \to \infty$. This indeed must be the case, because when $\alpha = 1$, our basin in Fig. 7 is becoming a constant depth basin, fully open to a deep ocean. Hence, one of limiting cases, that of a fully opened basin, appears naturally as a limiting case of the present theory. The values of R for the other limiting cases, a closed basin ($\alpha = 0$), with parabolic bottom, discussed by Chrystal (1905), can be seen in Fig. 8. There are no zeroes of the Legendre functions for $\alpha = 0$, due to the fact that in the closed basin there is a vertical displacement of water at the end $x = \ell$.

The shapes of the modes of oscillations corresponding to $\alpha = 0$ are presented as the top graphs in Fig. 9. It is seen that the solutions, corresponding to P_2 and P_4 are finite, while the solutions given by Q_1 and Q_3 tend to infinity at $x = \ell$. The last two solutions were described by Chrystal (1904) as "paradoxical seiches" and, indeed, they can not be present in any real situation, because they involve the infinite water displacement at the right end of the basin.

However, these "paradoxical seiches" become finite in amplitude and, hence, very real when the basin is not fully closed. For example, when $\alpha = 0.06$ the modal shape given by Q_3 has a zero vertical displacement at $x = \ell$, and Q_1 does not tend to infinity because for $\alpha = 0.06$ our domain is $[0, \sqrt{1-0.06}]^{1/2}$ where all values for Q_1 are finite.

We assign a particular significance to the modal shapes, giving zero (or nearly zero) vertical displacement at the sea side end ($x = \ell$ in Figure 7) when $\alpha > 0$ for the following reason.

In the outer region ($x > \ell$ in Fig. 7) there must exist the outgoing wave, propagating into the ocean, away from the basin, and carrying some energy of oscillations within the basin with the wave. The amplitude of this outgoing wave has to be matched to the amplitude of water oscillations in the basin at the point $x = \ell$. The higher is the amplitude of the modal shape at $x = \ell$, the larger will be the amount of seiche energy radiated to the ocean, hence, the more severe will be the damping of oscillation within the basin. The energy radiated towards the ocean will be minimal when amplitudes of modes at $x = \ell$ equal zero, hence the resonances within the basin will be the sharpest. Obviously, as the parameter α is approaching unity, the modal shapes of strong resonances are becoming very close to those for the fully open basin with constant depth. (Compare the cases of $\alpha = 0.8$ and $\alpha = 1$ on Fig. 9).

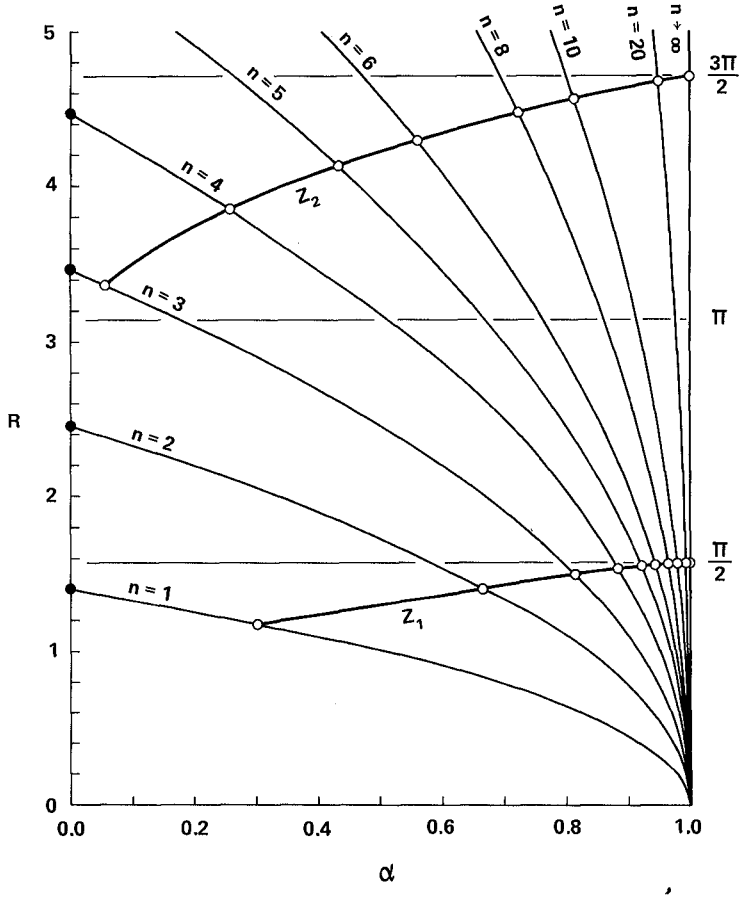

Figure 8. Non-dimensional Frequency of Oscillations R vs Relative Opening α

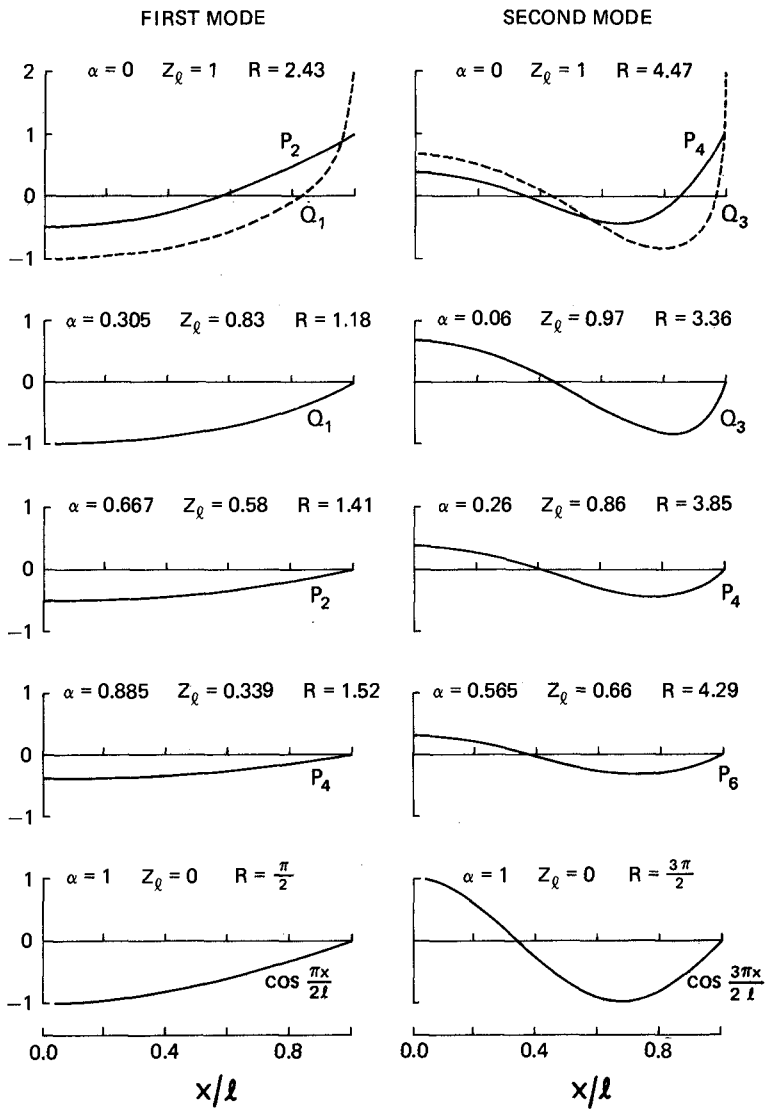

Figure 9. Modes of Water Oscillations in the Basin for Various Values of the Relative Opening α.

Returning back to Fig. 8, one can see, that the point $\alpha = 1$ is the point of condensation for zeroes of Legendre functions, hence for any $\alpha \simeq 1$ there exist a strong resonance plus an infinitely increasing number of weak resonances, also condensing near $\alpha = 1$.

It is clear now, that the second boundary condition, which we deliberately avoided to discuss so far, is:

$$\xi = 0 \quad \text{at } x = \ell \ (z = \sqrt{1-\alpha}) \tag{20a}$$

for strong resonances and

$$\xi < \infty \quad \text{at } x = \ell \ (z = \sqrt{1-\alpha}) \tag{20b}$$

for weak resonances.

In the Figure 9 the frequencies of strong resonances (in terms of non-dimensional values of R) together with the corresponding modal shapes are given. The case of a completely closed basin is also classified as a strong resonance, because there is no radiation of energy to the ocean when $\alpha = 0$.

Consulting again Fig. 8, we can see, that solid lines joining the zeroes display the interesting tendency to decrease, when α is decreasing from $\alpha = 1$. This means the frequencies of strong resonances are decreasing while the basin is becoming more closed. This result is in agreement with Tuck, (1980), who predicts a similar tendency for the basin of a constant depth with an infinitely thin barrier of a variable height ($0 < \alpha < 1$) at the point $x = \ell$. However, the essential difference is that in our case there exists a set of discrete parameters α , for which strong resonance is possible, while for the basin of a constant depth the strong resonances exist for any α within the continuum $0 \leq \alpha \leq 1$, if the outer basin (ocean) is deeper, than the inner basin.

5 Periods and damping of the strong resonances for the Western Australian Coastline

The average value of a reef height for the coastline corresponds to a value $\alpha = 0.3$. It is seen from Fig. 8, that this particular value is near the zeroes of the Legendre functions Q_1 and P_4, thus being capable of producing the two strong resonances, the modal shapes of which are depicted on Fig. 9.

The values R for $\alpha = 0.3$ are, as taken from Fig. 8, $R_1 = 1.18$; $R_2 = 3.84$, correspondingly for the first and second strong resonances. The average distance from reef chain to the shore can be taken as 5000 m, the periods of resonance oscillations are then, as follows from (18):

$$T = \frac{2\pi}{\omega} = \frac{2\pi\ell}{R(gh_o)^{1/2}} \tag{21}$$

Taking h_o = 10m and substituting the above values for R_1 and R_2 one finds: T_1 = 2688 sec = 44.8 min; T_2 = 826 sec = 13.8 min. In the spectral analysis of the large sea-level oscillations the period prominent was 40 min.

The current measurements were taken in the Mullaloo area, where the average distance of the reef chain from the shore is about 4500 m. Using the same values of R_1, R_2 as above, we would obtain from (21) the following periods: T_1 = 40.3 min, T_2 = 12.4 min. The last value is too small to be verified by our experimental data as the current meter records were sampled at 10 minute intervals. The results of the spectral analysis of currents gave a prominant period of 33 mins.

The difference of about 20% between the theoretical and experimental results is not bad when taking into account the crude estimates of water depth h and distance ℓ and the uneven bottom topography.

Our theoretical analysis gives consequently, reasonable prediction of the periods of sea-level oscillations. However, the damping was not considered in the theory and when the term "strong" resonance is used it does not give a quantitative idea yet of how strong the resonance is.

The quantitative measure, by which the resonance capabilities are usually judged, is the so-called "quality factor", denoted as Q (e.g. Miles and Munk, 1961). Resonances are considered sharp when Q >> 3-5. Sometimes the values Q up to 18 occur (e.g. Gill and Schumann, 1974). We give below an estimate of this factor for the recorded sea-level oscillations.

Considering one of the normal modes with a wave-length λ, we can write the maximum potential energy in this mode as

$$W = \frac{1}{4} \rho\, g\, \lambda\, A^2 \tag{22}$$

Let the amplitude A during one period T of free oscillations decrease by the value ΔA. The new value of maximum potential energy is

$$W-\Delta W = \frac{1}{4} \rho g \lambda [A^2 - 2A\cdot\Delta A + (\Delta A)^2] \tag{23}$$

Neglecting the second-order term $(\Delta A)^2$ and substracting eq (22) from eq (23) one obtains a loss in potential energy:

$$\Delta W = \frac{1}{2} \rho g \lambda A \cdot \Delta A \tag{24}$$

From eq (24) and eq (22), it follows that the relative energy loss ψ is twice the relative amplitude decrease δ during one cycle of oscillations.

$$\psi = \frac{\Delta W}{W} = \frac{2\Delta A}{A} = 2\delta \tag{25}$$

The values of ψ and δ are independent of λ, and hence independent of the shape and order of the normal modes. This means that damping of water oscillations can be studied without any knowledge of normal modes.

Let us denote by A_T the amplitude of sea-level oscillations after one period T has elapsed and consider the following supplementary relationship, which holds for small values of δ:

$$\ln \frac{A}{A_T} = \frac{\Delta A}{A} = \delta \tag{26}$$

From eq (26) it follows immediately the exponential law for the amplitude decay of free sea-level oscillations in the basin:

$$A_T = A \exp(-\delta) \tag{27}$$

The damping coefficient δ was estimated on the basis of the relationship (27) for the nine largest sea-level oscillation events recorded in Geraldton during the years 1963-1978.

Letting i be the event number and j be the order number of an amplitude with respect to the maximum, we can rewrite (27) as

$$A_{ij} = A_i \exp(-K_{ij}\ \delta_i) \tag{28}$$

where K_{ij} is the order number of jth amplitude in the event i and has the values 1, 2, 3... Taking the logarithm of (28), one obtains:

$$Y_{ij} = \ln A_{ij} - \ln A_i = -K_{ij}\ \delta_i \tag{29}$$

Linear regressions through the origin were fitted to individual sea-level oscillation events and estimates of the δ_i's were obtained from

$$\delta_i = -\frac{\sum_j K_{ij}\ Y_{ij}}{\sum_j K_{ij}^2} \tag{30}$$

The estimated values of δ_i ranged from 0.22 to 0.57, with a pooled value δ_c, obtained from combining sums of squares and cross products over events, of 0.29. From eq(25) it follows that the average relative energy loss ψ during one cycle of oscillations equals twice the value of δ_c, i.e. $\psi = 0.58$. The average resonance amplification factor Q can be estimated as:

$$Q = \frac{2\pi}{\psi} = \frac{6.28}{0.58} = 10.8 \qquad (31)$$

with a range from 5.5 to 14.3 in the individual sea-level oscillation events. The large value of Q obtained indicates that observed water oscillations are caused by resonance of the coastal waters in the nearshore basin between Perth and Geraldton, and the resonances are sharp indeed.

6 Conclusions

1) Sea-level oscillations between Perth and Geraldton, Western Australia, with periods of the order of 10-40 min. are caused by resonance of local waters in a basin between a shore and submerged reef chain.

2) The theory presented gives a reasonable agreement between observed and theoretical values of resonance periods.

3) Statistical analysis of recorded oscillations gives the average value of Q = 10.8, indicating that the resonances are sharp.

7 Acknowledgements

The authors are grateful to Mr. Austin from Public Works Department, Perth, for supplying the tidal records; Mr. T.J. Golding of CSIRO Division of Fisheries and Oceanography, Cronulla, for digitizing the current records and Mr. R. Symes of the Australian Survey Office, Perth for digitizing the tidal records.

8 References

ABRAMOWITZ, M. and STEGUN, I.A. (1970). Handbook of mathematical Functions. Dover, New York.

ALLISON, H.A. and GRASSIA, A. (1979). Sporadic sea-level oscillations along the Western Australian Coastline. Aust. J. Mar. Freshwater Res. 30(6), (in press).

CURRIE, R.G. (1976). The spectrum of sea level from 4 to 40 years. Geophys. J. Roy. Aston. Soc. 46, 513-520.

CHRYSTAL, G. (1904). Some results in the mathematical theory of seiches. Proc. Roy. Soc. Edin. XXV, 328-337.

GILL, A.E. and SCHUMANN, E.H. (1974). The generation of long shelf waves by the wind. J. Phys. Oceanogr. 4, 83-90.

HAMON, B.V. (1966). Continental shelf waves and the effect of atmospheric pressure and wind stress on sea-level. J. Geophys. Res. 71, 2883-93.

HAMON, B.V. (1976). Generation of shelf waves on the East Australian Coast by wind stress. Mémoires Société Royale des Sciences de Liége, 6^{e} Séme, tome X. pp 359-367.

LAMB, H. (1932). Hydrodynamics. Cambridge Univ. Press, London.

LE BLOND, P.H. and MYSAK, L.A. (1978). Waves in the ocean. Elsevier, Amsterdam.

MILES, J. and MUNK, W. (1961). Harbour paradox. J. Waterways and Harbour Div., ASCE, WW3, 111-130.

TUCK, E.O. (1980). The effect of a submerged barrier on the natural frequencies and radiation damping of a shallow basin connected to open water. J. Aust. Math. Soc. Series B. (in press).